Received: 27 November 2023 | Accepted: 14 December 2023

DOI: 10.1002/maco.202314209

ARTICLE

Materials and Corrosion

Long-term atmospheric corrosion rates of Zn55Al-coated steel

Dominique Thierry[1] | **Dan Persson**[1] | **Nathalie LeBozec**[2]

[1]Rise Research Institutes of Sweden, Stockholm, Sweden

[2]French Corrosion Institute, Brest, France

Correspondence
Nathalie LeBozec, French Corrosion Institute, 220 Rue Rivoalon, 29200 Brest, France.
Email: nathalie.lebozec@institut-corrosion.fr

Funding information
Industry; ArcelorMittal; voestalpine; SSAB Europe; Ternium; Tata Steel; Bluescope steel

Abstract

Hot-dip Zn55Al-coated steel samples have been exposed for up to 6 years at 11 different weathering sites, including marine, marine-industrial, acid-rain and dry atmospheres. From the mass loss measurements, Zn55Al metallic coating showed globally long-term good corrosion resistance in all weathering conditions compared with hot-dip Zn-0.2Al-coated steel (Z). Yet, weaker performance was observed on Zn55Al in high SO_2 polluted atmosphere, particularly when combined with seawater aerosols. This is explained by a more acidic surface condition linked to high SO_2. Although the extent of corrosion in this phase was different at the different sites, the final corrosion products formed after 6 years were rather similar at all sites. This consists of hydrous aluminium sulphate or hydrous aluminium hydroxy sulphate and, probably also a smaller amount of sulphate-containing zinc corrosion products or Al/Zn products.

KEYWORDS

atmospheric corrosion, hot-dip zinc-coated steel, zinc aluminium

1 | INTRODUCTION

Hot-dip galvanised zinc (Z) and zinc-55% aluminium (Zn55Al)-coated steel are widely used in the construction industry for various applications. In particular, these materials are used for roofing and siding of metallic constructions. The atmospheric corrosion of zinc has been extensively studied and the progress has been summarised in several recent reviews.[1–3] The composition of corrosion products formed on zinc in different environmental conditions has been studied by numerous authors.[4–10] This includes the sequence of formation of corrosion products formed under marine and industrial environments.[7] In recent work, the long-term behaviour of hot dip galvanised steel has been reported by Persson et al.[11] Zn55Al contains about 1.5% Si, which is added to prevent an exothermic reaction at the coating overlay/substrate steel interface. The metallurgy of Zn55Al has been described in a review by Marder.[12] The coating consists of beta aluminium dendrites (about 80% in volume and containing approximately 18% zinc), zinc-rich interdendritic regions containing about 22% aluminium and a fine dispersion of Si particles. The interdendritic region contains also many precipitates and several phases.[13] One of the phases of the interdendritic areas is aluminium-rich containing zinc and the other is zinc-rich containing aluminium.[13] Due to its microstructure, the corrosion of Zn55Al will be selective. As both zinc and aluminium are reactive metals, the selective dissolution of the different phases may highly depend upon exposure conditions and local chemistry at the interface coating/atmosphere. This was recently demonstrated by Zhang et al.,[14] showing that the release rate of zinc and

aluminium from Zn55Al depends on the chloride concentration due to differences in the stability of Al_2O_3 in artificial rainwater and marine aerosols.

Palma et al. studied the atmospheric corrosion of Zn55Al-coated steel in various types of atmospheres in Spain, Brazil and Portugal.[15] The results were compared with galvanised steel (Z) after 1, 2, 3 and 5 years of exposure. A better performance of Zn55Al was observed at all locations. However, both materials were passivated using chromium and phosphorus solutions making the comparison of the behaviour more difficult, in particular for short-term exposure times. Moreover, in a recent article, it was shown that the effect of passivation for galvanised steel could still be observed after at least 3 years of exposure at various locations worldwide.[11] Palma et al. also indicated that the attack starts in the interdendritic phases of the coating, mainly affecting the zinc in the alloy.[15] Similar observations were done by Qui et al. based on marine exposures.[16] However, based on 5-year exposure data in Brazil, Moreira et al. observed that the corrosion of the Zn55Al coating occurs through the aluminium-rich phases of the interdendritic areas.[13] The preferential corrosion of interdendritic areas was also observed during short-term exposure in a marine environment in Sweden with the formation of AlOOH, $Al(OH)_3$, an aluminium sulphate of unknown identity and the parallel formation of primarily ZnO, hydrozincite and simonkolleite.[16] Upon longer times of exposure, crystalline $Al(OH)_3$ was detected. Different corrosion products were reported by Persson et al. based on Fourier transform infrared spectroscopy (FTIR) microscopy.[17] In that case, $NaZn_4(SO_4)Cl(OH)_6{\cdot}6H_2O$ was located in certain spots on the surfaces, for example, the anodic areas, while the $Zn_{0.71}Al_{0.29}(OH)_2(CO_3)_{0.145}{\cdot}xH_2O$ was formed in the cathodic regions outside the former. These results confirmed the observations made by Palma et al. and Qui et al., indicating a preferential dissolution of zinc in the interdendritic areas, with the Al dendrites acting as the cathode.[15,16] It should be noticed that in agreement with Persson et al., zinc aluminium carbonate ($Zn_6Al_2(OH)_{16}CO_3{\cdot}4H_2O$) was also observed in the corrosion products upon exposure to salt spray test [18] and under wet storage conditions.[19]

Hence, despite the available literature on the corrosion behaviour of Zn55Al, there are still many questions that need further research. In particular, the performance of Zn55Al compared with hot dip galvanised steel under various exposure conditions as well as the nature of the protective patina formed needs further attention.

The objective of this investigation was to determine the long-term corrosion behaviour of Zn55Al under a wide range of climatic conditions worldwide. In addition, the corrosion products formed after different times of exposure and exposure conditions will also be discussed.

2 | EXPERIMENTAL

2.1 | Materials

Table 1 gives the chemical composition of the different coatings used as well as the coating weight and the thickness of the steel. For Z, the density of zinc, for example, 7.14 g/cm³ was taken while for Zn55Al, the density of 4.61 g/cm³ was calculated taking into account the fraction of aluminium, silicium and zinc in the coating.

These materials have been provided in large panels, which have been cut using a shearing machine. Panels of 150 × 100 mm were used at all exposure sites. Before exposure, a cleaning step consisting of two periods of 10 min in a heptane (C_7H_{16}) bath under ultrasonic agitation was performed. Once cleaned, the corrosion samples have been dried in a desiccator for at least 24 h. Then, each corrosion sample was weighed using a laboratory balance (Sartorius CPA224S, +/-0.1 mg). A masking tape had been applied on the back and the edge of these samples.

In addition, carbon steel (e.g., DC01, EN 1.0330) and pure zinc (Z1 grade) have been exposed for 1 year at each field site to determine the corrosivity class according to ISO 9223.

2.2 | Exposure sites

Eleven exposure sites located around the world have been selected to obtain a broad range of climatic conditions, for example, marine, marine industrial, marine tropical, and acid rain atmospheres. The exposure sites are presented in Table 2. The corrosivity of steel and zinc according to ISO 9223 is also given. These measurements were performed during the first year of exposure and repeated during the second year. For all sites except Bohus Malmön Kvarnvik,

TABLE 1 Metallic coatings.

Label	Coating	Zinc [%]	Aluminium [%]	Silicium [%]	Density [g/cm³]	Nominal coating weight [g/m²]	Steel thickness [mm]
Z180	Z	99.8	0.2	-	7.14	180	1.4
AZ185	Zn55Al	43.4	55	1.6	4.61	185	1

TABLE 2 Locations and characteristics of exposure sites.

	Exposure site	Distance to the sea (m)	Average Chloride deposition [mg/m^{2}day]	Average SO_2 [μg/m^3]	Corros. Class ISO 9223		Classification
					C-steel	Zinc	
Europe	Bohus Malmön Kattesand (Sweden)	300	220	<1	C3	C3	Marine
	Bohus Malmön Kvarnvik (Sweden)	<5	750	36[a]	CX (C5)	C5 (C3)	Marine[a]
	IJmuiden (The Netherlands)	2600	26	6	C3	C3	Marine/Industrial
	Brest (France)	<5	1064	<1	C5	C3	Marine
Asia	Qingdao (China)	10	15	30	C2	C3	Marine/Industrial
	Jiangjin (China)	~900 km	nd	218	C3	C3	Industrial/Urban
	Wanning (China)	100	77	12	CX	C4	Marine
	Singapore	10	18	25	C3	C3	Marine/Urban
	Bangkok (Thailand)	35 km	2	1	C2	C2	Urban
Middle East	Dubai (Emirates)	2000	84	11	C2	C4	Marine/Urban
USA	Daytona Beach	100	174	<1	CX	C4	Marine

Note: Corrosivity class according to ISO 9223. The data were obtained during the first year of exposure. Values between brackets represent the second year of exposure and are only shown if different from the first year.

[a]During the first year of exposure, a very high SO_2 value was measured; at that time, this field station should be considered as marine/industrial. During years 2–6, the SO_2 value was more in a normal range for this field station below 1 μg/m^3.

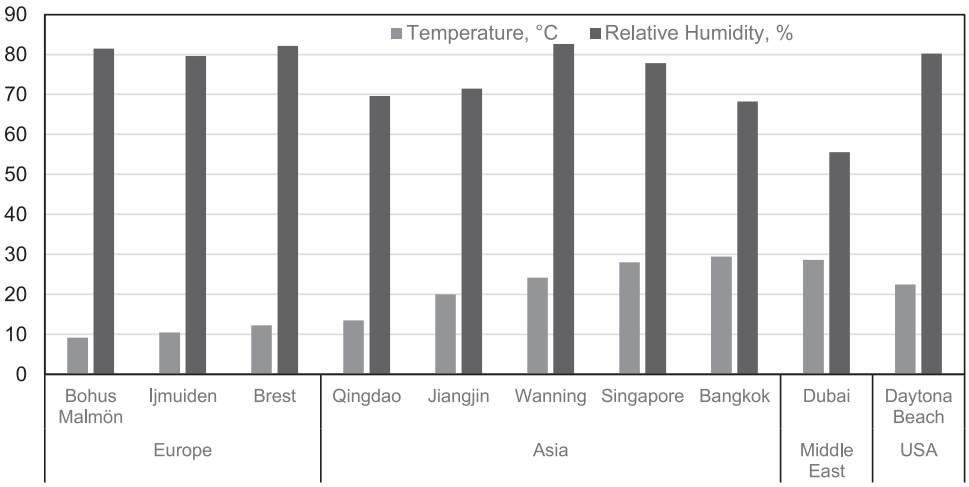

FIGURE 1 Mean temperature and relative humidity at different sites (average values over 6 years).

the results were in line with previous results. In the case of Bohus Malmön Kvarnvik, very high corrosivity was observed in the first year of exposure, probably linked to local pollution (with leakage of SO_2). The values measured in the second year of exposure at this site were more in line with previous data.

From Table 2, it is also clear that chloride deposition varied from about 2 to above 1000 mg/m^{2}day whereas the SO_2 content varies from about 1 to 218 μg/m^3. Figure 1 shows the mean relative humidity (RH) and temperature during the 6 years of exposure. As inferred from Figure 1, the mean temperature (T) varied from 10 to 30°C. The mean RH showed less variation with the driest site being located in Dubai. More information concerning RH and T of these sites during the exposure period may be found elsewhere.[11]

For all sites, the samples have been exposed at the inclination of 45° to the horizontal and facing South or the corroding source (sea).

2.3 | Weight loss measurements

Three replicates of each material have been removed after 1, 2, 4 and 6 years of exposure. The samples were brushed to remove nonadherent corrosion products, rinsed in flowing water and the corrosion products were removed by pickling according to ISO 8407. Clark solution was used for steel reference samples. Glycine was used for zinc and hot-dip galvanised steel (Z). Chromic acid was used for Zn55Al. The composition of the different pickling solutions is given in Table 3.

2.4 | Analysis of corrosion products

Infrared reflection absorption spectra (IRRAS) of the corrosion products were measured using a Bruker Vertex 70 spectrometer with reflection accessory (Seagull™, Harrick Scientific), using p-polarised light (KRS-5 wire grid polariser) and an angle of incidence of 10°C. The spectrometer was equipped with Bruker FM beamsplitter for measurements on Mid-IR and Far-IR spectral regions. The measurements were performed in the region 200–4000 cm^{-1} using a resolution of 8 cm^{-1}. An Au-mirror was used as background for the FTIR measurements.

TABLE 3 Pickling solutions.

Designation	Composition (for 1 L)
Glycine	saturated solution of glycine (NH_2CH_2COOH)
	Distilled water to make 1000 mL
Chromic acid	100 g of chromium trioxide (CrO_3), 10 g of silver nitrate ($AgNO_3$)
	Distilled water to make 1000 mL
Clark's	1000 mL of hydrochloric acid (HCl,ρ = 1,19 g/mL)
	20 g of antimony trioxide (Sb_2O_3)
	50 g of tin(II) chloride ($SnCl_2$)

2.5 | SEM-EDS measurements

Scanning electron microscopy observations (SEM) were performed using an LEO 1530 with Gemini column, upgraded to a Zeiss Supra 55. The energy dispersive X-ray spectroscopy (EDS) detector was a 50 mm^2 X-Max sSilicon drift detector (SDD) from Oxford Instruments. SEM-EDS of cross-sections was performed after mounting samples in two-component cold-hardening epoxy resin and sequential polishing in ethanol. Exposed sample surfaces were examined with SEM without further sample preparation.

3 | RESULTS AND DISCUSSION

3.1 | Mass loss measurements

Figure 2 shows the mass loss of AZ185 after 1, 2, 4 and 6 years of exposure at the different field sites. From the results, it is clear that the highest mass loss was

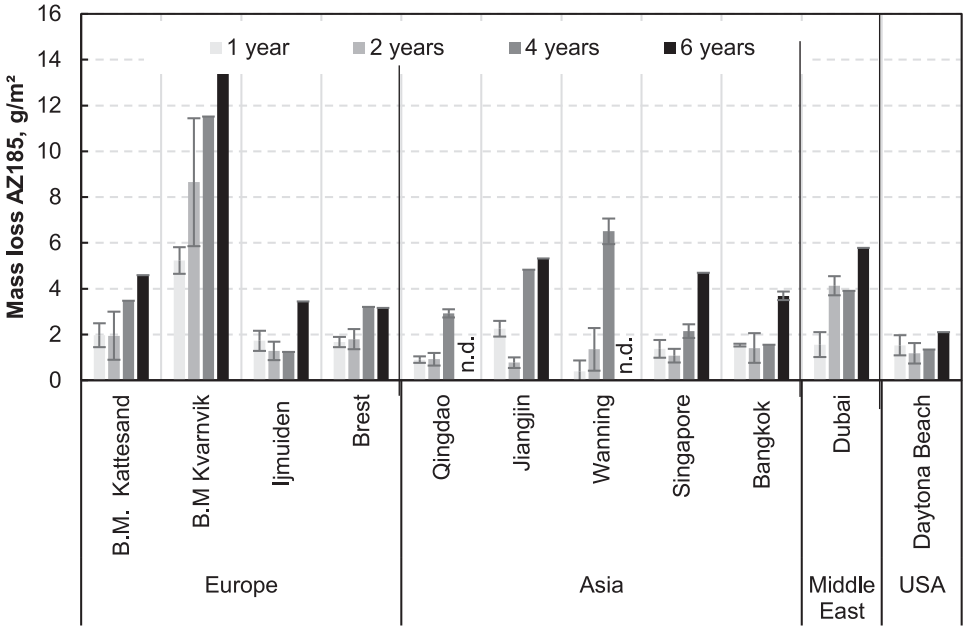

FIGURE 2 Mass loss of AZ185 after 1, 2, 4 and 6 years of exposure at different sites. n.d., no data.

measured in the marine atmosphere of Bohus Malmön Kvarnvik (Sweden). It should be noticed that this is linked to the very high SO_2 deposition rate measured at this location during the first year of exposure. Indeed, the first year of exposure represents about 1/3 of the total mass loss measured after 6 years of exposure. As further observed in Figure 2, the mass loss at Bohus Malmön Kvarnvik was much higher than that observed at Bohus Malmön Kattesand. As both stations are only distant of 1 km, the RH and temperature are similar (see Figure 1). Hence, the difference in corrosivity is related to the chloride and SO_2 deposition levels (see Table 2). However, it should be noticed that no direct correlation could be found between the climatic parameters given in Table 2 and Figure 1, and the mass loss measured after 6 years at the different sites. Figure 3 shows the mass loss of Z180 compared with AZ185 after 4 and 6 years of exposure at the different sites while the ratio of the mass loss between Z180 and AZ185 is plotted in Figure 4. The higher the ratio, the better the performance of AZ185 at a given site. The ratio after 6 years of exposure ranged from about 7.5 at Bohus Malmön Kvarnvik to above 30 at Daytona Beach. This is in agreement with previous works.[15–17] This also indicates the very good long-term performance of Zn55Al under different types of weathering conditions as observed elsewhere.[20] It should be noted that the lowest ratios were measured at Bohus Malmön Kvarnvik and Jianging for which high SO_2 levels were measured (in particular at Bohus Malmön Kvarnvik during the first year of exposure). Hence, the less good performance of AZ185 at these stations compared with for instance pure marine conditions with no or very low SO_2 levels (e.g., Brest and Daytona Beach) may be related to more acidic conditions linked to SO_2 deposition.

3.2 | Corrosion products

FT-IRRAS spectra of the surface recorded after different exposure times at the marine site of Brest and the marine/industrial site of Qingdao (Marine industrial) are shown in Figures 5 and 6. Initially, broad bands are seen around 1630 and 3400 cm^{-1}. The latter band is due to O–H stretching bands due to hydroxyl groups and/or water in the corrosion products, while the band at 1630 cm^{-1} is due to water. A broad band from 900 to 1100 cm^{-1} with a maximum of 1015 cm^{-1} has probable contributions from both hydroxyl groups and sulphate ions. With increasing exposure time, the intensities of the spectra increase, and more details are seen in the spectra. It can be noticed that a fine structure of the OH/SO_4^{2-} band develops with exposure time with the appearance of a band at 550 cm^{-1}after 2 and 6 years of exposure. An SEM image and EDS analysis of a cross-section of a sample exposed 6 years at Brest is shown in Figure 7. It is seen that the zinc-rich phases are preferentially attacked and the corrosion products containing chlorine and sulphur are formed where the zinc-rich phases are located. In the corroded parts, closer to the outer surface, high oxygen content is seen and low zinc content compared with the uncorroded parts of the zinc-rich phases. The latter appear

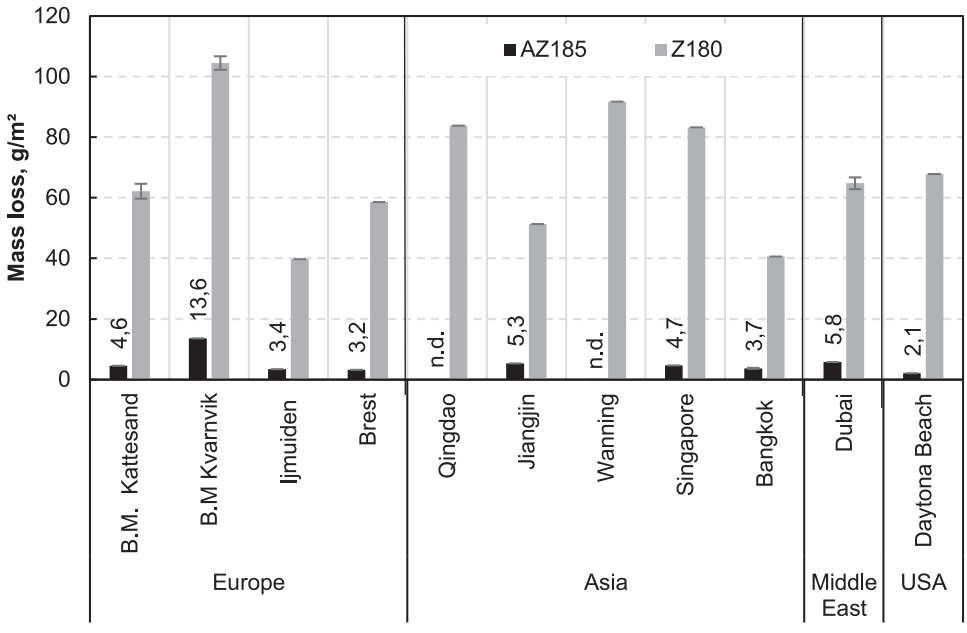

FIGURE 3 Comparison of mass loss of AZ185 and Z180 after 6 years of exposure at different sites. n.d., no data.

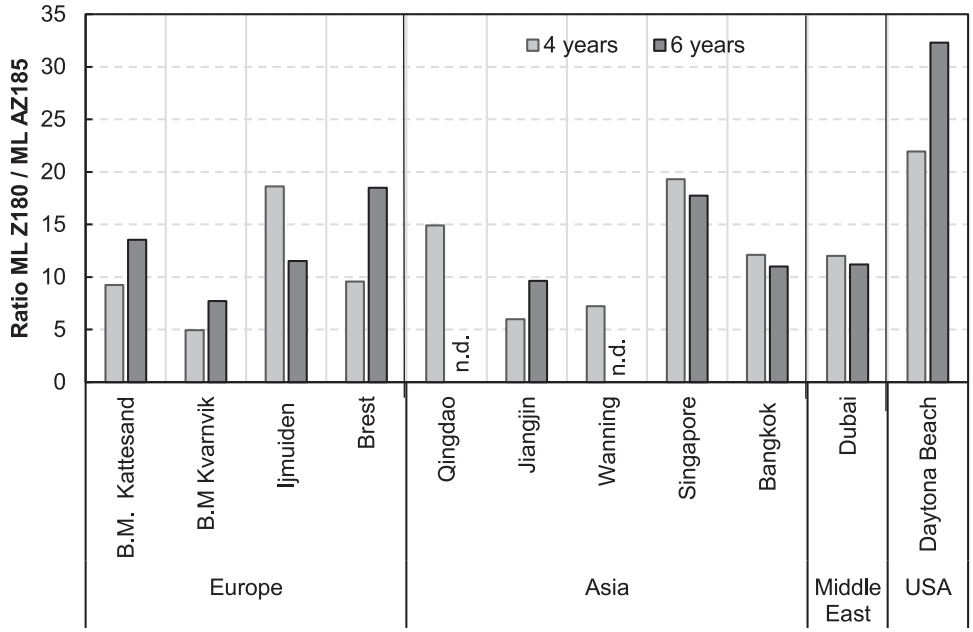

FIGURE 4 Ratio of mass loss Z180/AZ185 after 4 and 6 years of exposure at different sites.

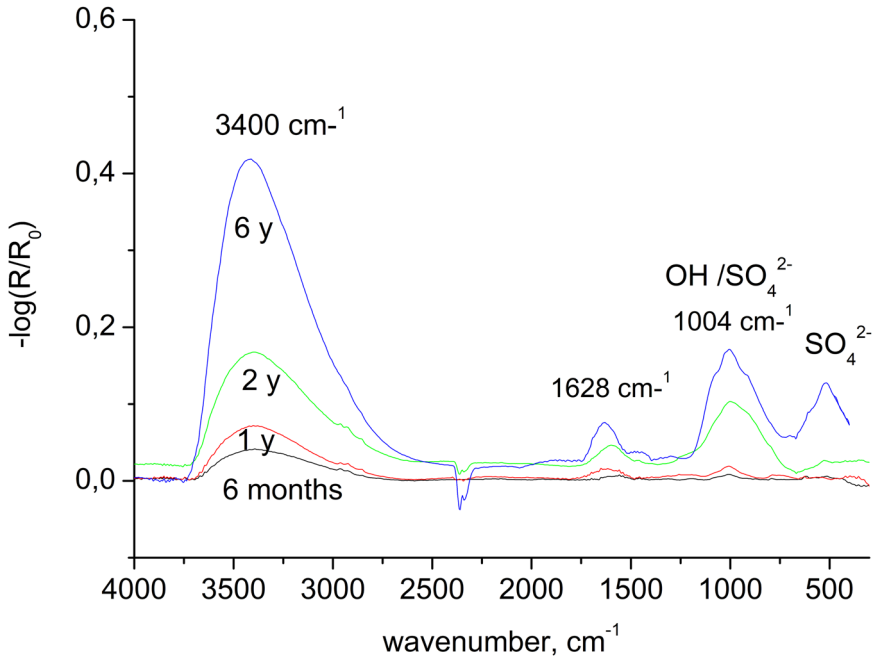

FIGURE 5 Infrared spectra of AZ185 after 0.5, 1, 2 and 6 years of exposure in Brest. [Color figure can be viewed at wileyonlinelibrary.com]

as white areas in the SEM image. The EDS point analysis and the SEM-EDS images in Figures 7 and 8 show that both chlorine and sulphur are present in the corroded areas. While chlorine is located mainly inside corroded zones, sulphur is accumulated both on the outer surface and in the corroded zones inside the metallic coating. The oxygen content is low in the aluminium-rich phase as it is largely unaffected by corrosion. The FTIR spectra are measured by the reflection of the infrared light on the outer surface and represent mainly the composition of the corrosion product on the surface and probably only the outer parts of the corrosion-affected zones.

The cross-section analysis of samples exposed in Qingdao in Figure 9 shows that zinc-rich phases are preferentially attacked similarly to the samples exposed at the site of Brest. However, the zinc-rich phases are completely corroded in this case with the formation of sulphur-containing corrosion products where the zinc-rich phases were located. As observed in Table 2, Qingdao has a rather high concentration of SO_2 (e.g., 30 $\mu g/m^3$). Hence, the amount of sulphur

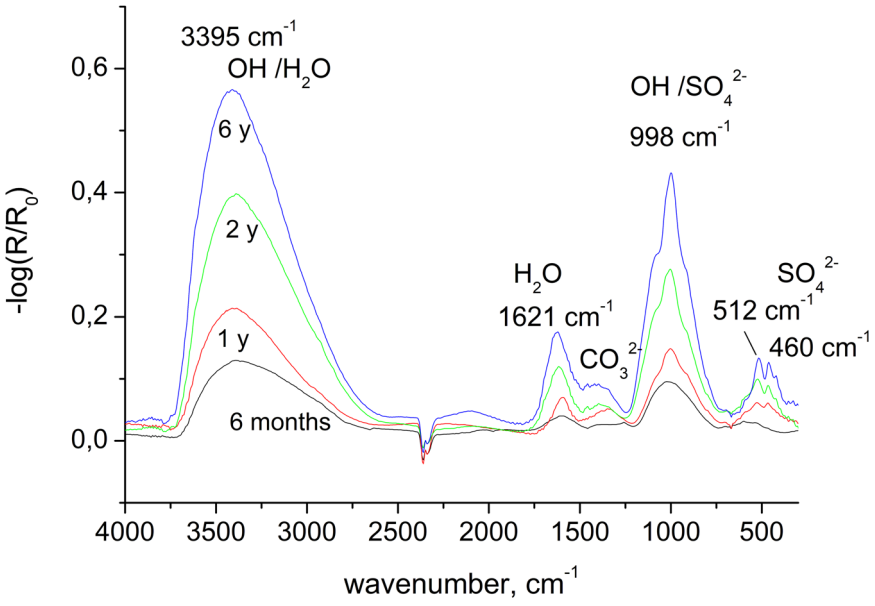

FIGURE 6 Infrared spectra of AZ185 after 0.5, 1, 2 and 6 years of exposure in Qingdao. [Color figure can be viewed at wileyonlinelibrary.com]

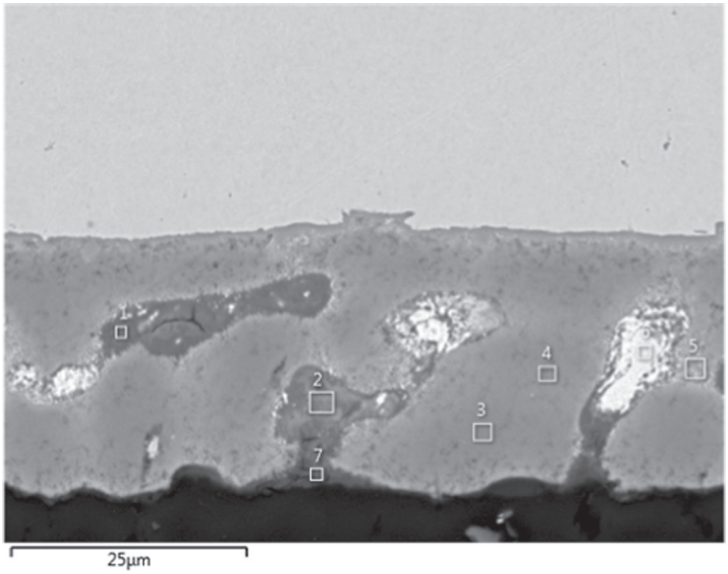

FIGURE 7 Scanning electron microscopy (SEM) image of cross-section of AZ185 after 6 years of exposure in Brest.

Element (Wt%)	1	2	3	4	5	6	7
O	20.45	24.80	1.11	1.31	1.81	0.84	40.33
Al	43.05	22.91	69.07	65.50	46.96	5.06	23.77
Si	0.25	0.38	0.53	0.59	0.32	0.06	0.44
S	3.17	3.72					2.08
Cl	8.87	2.80		0.06			0.72
Zn	22.99	43.77	28.70	31.71	49.63	92.29	21.48

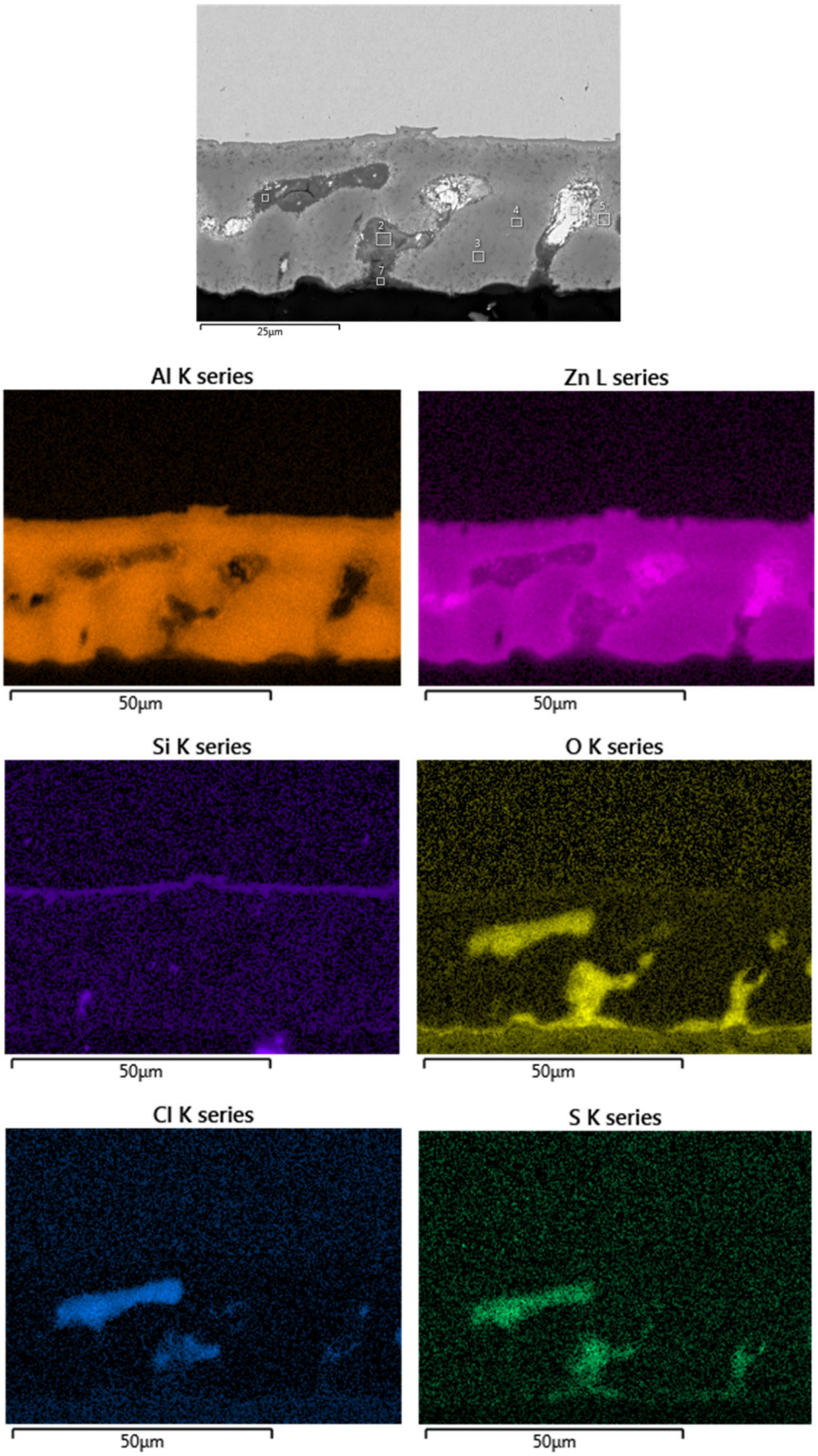

FIGURE 8 Scanning electron microscopy-energy dispersive X-ray spectroscopy (SEM-EDS) elemental images of cross-section of AZ185 after 6 years of exposure in Brest. [Color figure can be viewed at wileyonlinelibrary.com]

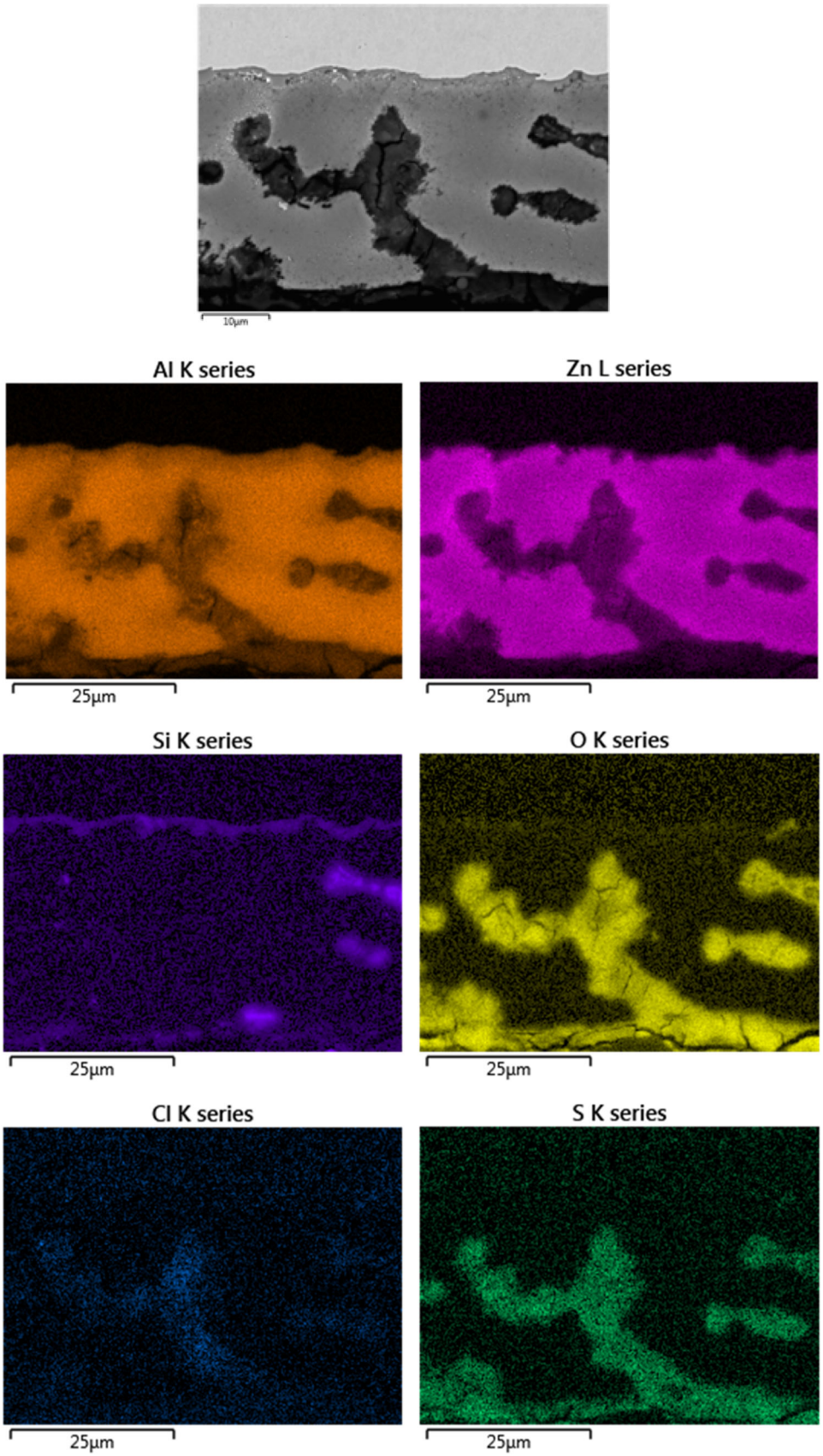

FIGURE 9 Scanning electron microscopy-energy dispersive X-ray spectroscopy (SEM-EDS) elemental images of cross-section of AZ185 after 6 years of exposure in Qingdao. [Color figure can be viewed at wileyonlinelibrary.com]

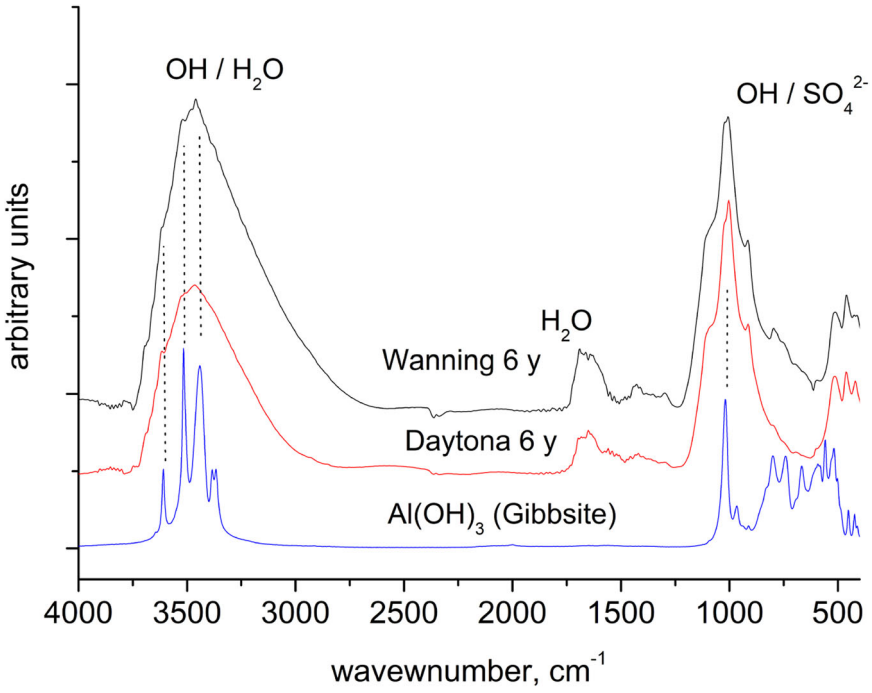

FIGURE 10 Infrared spectra of AZ185 after 6 years of exposure in Wanning and Daytona. Comparison with reference transmission spectrum of $Al(OH)_3$ (Gibbsite). [Color figure can be viewed at wileyonlinelibrary.com]

observed in Figure 9 is linked to the high deposition rate of SO_2 and the subsequent acidification of the surface. Chloride is present in the corroded zinc-rich phases. The surface is covered with sulphur-containing corrosion products.

A comparison of FTIR spectra obtained after 6 years of exposure shows that corrosion products are similar irrespective of exposure site. The spectra are all dominated by bands due to hydroxyl groups, sulphate and water. The formation of sulphate-containing corrosion products is consistent with the presence of sulphur in the corroded zinc-rich phases and on the outer surface of the coating. As shown in Figure 10, the O–H stretching band at 1000 cm^{-1} becomes finer after long exposure times on several exposure sites. This is consistent with the formation of gibbsite ($Al(OH)_3$) after prolonged exposures, as highlighted in Figure 10, when compared with the FTIR spectrum of this mineral.

Detailed assignment of the infrared spectra is difficult but they likely consist of Al/Zn-based corrosion products. Typical corrosion products that may form on Al/Zn-coated steel are shown in Table 4. However, the results from the FTIR measurements and SEM-EDS show that the corrosion products in the outer parts contain aluminium, zinc and sulphur with the latter in the form of sulphate. The zinc content is considerably lower compared with aluminium in corrosion products. From the results, it is suggested that the corrosion products largely consist of hydrous aluminium sulphate or hydrous aluminium hydroxy sulphate and, probably also a smaller amount of sulphate-containing zinc corrosion products or Al/Zn products. Chloride-containing Zn and Al corrosion products, such as simonkolleite and gordaite, can be located mainly in deeper corrosion attacks of the zinc-rich phases. Aluminium hydroxide is probably present on the outer parts of the corrosion layer

TABLE 4 Some possible corrosion products on Zn55Al alloy coatings after atmospheric exposure, their chemical formula and abbreviations.

Name	Chemical formula
Hydrozincite	$Zn_5(OH)_6(CO_3)_2$
Simonkolleite	$Zn_5(OH)_8Cl_2{\cdot}H_2O$
Gordaite	$NaZn_4(SO_4)(OH)_6Cl{\cdot}6H_2O$
Zinc hydroxy sulphate	$Zn_4(OH)_6\ SO_4{\cdot}3H_2O$
	$Zn_4(OH)_6\ SO_4{\cdot}5H_2O$
Zincite	ZnO
Aluminium hydroxy	$Al_2(OH)_4(SO_4)\ 7H_2O$
Sulphate	$Al_4(OH)_{10}(SO_4)\ 4H_2O$
Aluminium sulphate	$Al_2(SO)_3{\cdot}xH_2O$
Hydrated	
Aluminium hydroxide	$Al(OH)_3$
Aluminium oxy hydroxide	AlOOH
Layered double hydroxide	$M(II)_xM(III)_y(A)_m(OH)_n{\cdot}zH_2O$
	$M(II) = Zn^{2+}$
	$M(III) = Al^{3+}$
	$A = CO_3^{2-}, Cl^-, SO_4^{2-}$
	$Zn_2Al(OH)_6(CO_3)_{1/2}\ zH_2O$

and is formed to a larger extent probably after prolonged exposure when metallic zinc-rich phases are consumed. Small amounts of carbonate-containing corrosion products can be present in some exposure sites. In a previous study, the formation of sulphate-containing corrosion products was seen, but in addition to zinc hydroxy carbonate and Zn/Al hydroxy carbonate (LDH).[17] However, aluminium hydroxide was not detected in that study.

4 | CONCLUSIONS

The following conclusions may be drawn:

- Zn55Al-coated steel shows very good long-term performance under different types of weathering conditions, including pure marine, marine/industrial and industrial atmospheres with corrosivity classes ranging from C2 to CX for steel.
- The ratio in performance of Zn55Al compared with Z was in general better at the field site with no or low SO_2 in the air. This was explained by acidic conditions linked to SO_2 deposition that may attack the aluminium-containing phase.
- The zinc-rich phases were preferentially attacked and the corrosion products containing chlorine and sulphur were formed where the zinc-rich phases were located.
- Although the extent of corrosion in the zinc-rich phase was different at different field sites, rather similar corrosion products were observed at all sites. These consisted of hydrous aluminium sulphate or hydrous aluminium hydroxy sulphate and, probably also a smaller amount of sulphate-containing zinc corrosion products or Al/Zn products. Aluminium hydroxide was probably present on the outer parts of the corrosion layer. It was formed after prolonged exposure (due to higher corrosion rates) when metallic zinc-rich phases were over.

ACKNOWLEDGEMENTS

ArcelorMittal, voestalpine, SSAB Europe, Ternium, Tata Steel and Bluescope steel are acknowledged for the financial support. All the site managers are thanked for their support, as well as Jean Michel Hamoignon (FCI) for the technical help in Dubai, Brest and Bohus-Malmön.

DATA AVAILABILITY STATEMENT

The data that support the findings of this study are available from the corresponding author upon reasonable request.

ORCID

Nathalie LeBozec http://orcid.org/0000-0002-1753-9972

REFERENCES

[1] C. Leygraf, T. Graedel, *Atmospheric Corrosion*, Wiley, New York **2000**.
[2] I. Odewall Wallinder, C. Leygraf Corrosion **2017**; *73*, 1060
[3] D. Thierry, D. Persson, N. Le Bozec, *Atmospheric Corrosion of Zinc and Zinc Alloyed Coated Steel, Encyclopedia of Interfacial Chemistry*, Elsevier, Amsterdam **2017**.
[4] D. de la Fuente, J. G. Castaño, M. Morcillo, *Corros. Sci.* **2007**, *49*, 1420.
[5] R. Grauer, *Materials and Corrosion* **1980**, *31*, 837.
[6] J. J. Friel, *Corrosion* **1986**, *42*, 422.
[7] I. Odnevall, C. Leygraf, *Corros. Sci.* **1993**, *34*, 1213.
[8] I. Odnevall, C. Leygraf Atmospheric Corrosion, *ASTM STP 1239* (Eds. W. W. Kirk, H. H. Lawson), American Society for Testing of Materials, Philadelphia **1995**, pp. 215.
[9] I. S. Cole, W. D. Ganther, S. A. Furman, T. H. Muster, A. K. Neufeld, *Corros. Sci.* **2010**, *52*, 848.
[10] Z. Cui, X. Li, K. Xiao, C. Dong, Z. Liu, L. Wang, *Corrosion* **2014**, *70*, 731.
[11] D. Persson, D. Thierry, O. Karlsson, *Corros. Sci.* **2017**, *126*, 152.
[12] A. R. Marder, *Prog. Mater. Sci.* **2000**, *45*, 191.
[13] A. R. Moreira, Z. Panossian, P. L. Camargo, M. F. Moreira, I. C. Silva, J. E. R. de Carvalho, *Corros. Sci.* **2006**, *48*, 564.
[14] X. Zhang, T. N. Vu, P. Volovitch, C. Leygraf, K. Ogle, I. O. Wallinder, *Appl. Surf. Sci.* **2012**, *258*, 4351.
[15] E. Palma, J. M. Puente, M. Morcillo, *Corros. Sci.* **1998**, *40*, 61.
[16] P. Qui, C. Leygraf, I. Odnevall Wallinder, *Mater. Chem. Phys.* **2012**, *133*, 419.
[17] D. Persson, D. Thierry, N. LeBozec, *Corros. Sci.* **2011**, *53*, 720.
[18] P. R. Seré, M. Zapponi, C. Elsner, A. Di Sarli, *Corros. Sci.* **1998**, *40*, 1711.
[19] I. Odnevall Wallinder, W. He, P. E. Augustsson, C. Leygraf, *Corros. Sci.* **1999**, *41*, 2229.
[20] H. E. Townsend, A. R. Borzillo Mater, *Performance* **1987**, *26*, 37.

How to cite this article: D. Thierry, D. Persson, N. LeBozec, *Mater. Corros.* **2024**, 1–11. https://doi.org/10.1002/maco.202314209